

## **Study of Protective Iron Carbonate Layer Dissolution in a CO<sub>2</sub> Corrosion Environment**

Yang Yang<sup>1</sup>, Bruce Brown and Srdjan Nesic  
Institute for Corrosion and Multiphase Technology  
342 West State St.  
Athens, OH, 45701  
U.S.A.

### **ABSTRACT**

As a corrosion product, iron carbonate can protect underlying mild steel from rapid corrosion in a CO<sub>2</sub> aqueous environment. Chemical dissolution of a protective iron carbonate layer was investigated in a glass cell using a rotating cylinder electrode. It was observed that corrosion rate of the underlying steel increased as a consequence of the dissolution of protective iron carbonate layer due to exposure to an under-saturated solution. With the capability of in situ measurement of mass change on the surface, the electrochemical quartz crystal microbalance (EQCM) was also employed to directly monitor the iron carbonate dissolution rate. EQCM results indicated that iron carbonate dissolution was not affected by mass transfer. A mechanism of iron carbonate dissolution was proposed and the kinetics expression was obtained.

Key words: CO<sub>2</sub> corrosion, mild steel, iron carbonate layer, dissolution, rotating cylinder electrode, quartz crystal microbalance

### **INTRODUCTION**

In the oil and gas industry, internal corrosion of mild steel pipelines is commonly encountered during production and transportation. Iron carbonate is the main corrosion product layer in a CO<sub>2</sub> aqueous environment. The formation of an iron carbonate layer can protect the steel from rapid corrosion by acting as a diffusion barrier for cathodic species and also by covering portions of the steel surface and blocking the iron dissolution reaction. Partial removal of the protective iron carbonate layer can lead to severe localized corrosion aggravated by the galvanic effect established between carbonate layer-covered and bare steel areas<sup>1</sup>. Therefore, it is very important to understand the mechanisms of protective iron carbonate layer removal. It was previously reported that the protective iron carbonate layer cannot be removed by the mechanical forces exerted by flow alone<sup>2</sup>. Chemical dissolution is

---

<sup>1</sup> Current affiliation: BP Exploration and Production, 501 Westlake Park Blvd., Houston, TX, 77079, U.S.A

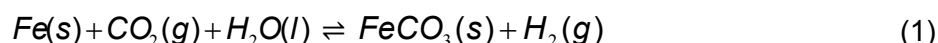
©2013 by NACE International.

Requests for permission to publish this manuscript in any form, in part or in whole, must be in writing to NACE International, Publications Division, 1440 South Creek Drive, Houston, Texas 77084.

The material presented and the views expressed in this paper are solely those of the author(s) and are not necessarily endorsed by the Association.

another possible mechanism for iron carbonate protective layer damage that can lead to exposure and rapid corrosion of the mild steel substrate.

The overall electrochemical reaction that occurs in corrosion of mild steel exposed in a CO<sub>2</sub> aqueous environment can generally be expressed as reaction (1):



which is composed of an anodic reaction (iron dissolution) and a cathodic reaction (hydrogen reduction) combined with intermediate chemical reaction steps involving the carbonic species. Iron carbonate precipitation/dissolution reaction can be written as reaction (2):



Iron carbonate dissolves when the saturation level of the solution is below 1 (undersaturation), and precipitates when it is above one (supersaturation).

In an early study on the subject, the effect of iron carbonate dissolution on mild steel corrosion in CO<sub>2</sub> environment was documented by Dugstad<sup>3</sup>. He illustrated the interaction between corrosion rate and solution saturation level and used it to explain the initiation of mesa attack at high temperatures. Ruzic et al.<sup>4</sup> investigated the effect of iron carbonate dissolution on CO<sub>2</sub> corrosion. Based on the experimental results, a mass transfer controlled mechanism was proposed. However, the procedure of iron carbonate layer formation in their study involved anodic polarization for 4 hours with large current, which resulted in an unrealistic iron carbonate layer.

In the geological field, since carbonates are very commonly found as minerals, extensive studies have been made to understand the mechanism of dissolution<sup>5-9</sup>. Dissolution kinetics of iron carbonate was studied for a range of temperatures and pressures<sup>10-16</sup>. The effects of environmental conditions, such as the presence of oxygen<sup>5,6</sup> and chromate<sup>17</sup>, were also investigated. It was suggested that the dissolution of iron carbonate was a surface reaction controlled process. In all of the studies, samples of siderite mineral were used, in the form of a single crystal, powder or as a polycrystalline substance.

Despite the fact that some work was done related to iron carbonate dissolution in the geological systems, there is very little information available which is directly related or applicable to CO<sub>2</sub> corrosion and specifically to conditions seen in the oil and gas industry. One major difference between these two applications is related to the presence of a steel substrate in corrosion which is not present in the geological systems. The nature and amount of minor components (contaminants) in solid iron carbonate are very different for the two systems. Finally, in the geological systems the direct effect of flow was not an important focus, whereas in pipeline corrosion it is.

## EXPERIMENTAL METHODS

In the present work, iron carbonate layer dissolution was first monitored using a SEM. Subsequently, quantitative studies were made using a glass cell with rotating cylinder electrode (RCE) setup and another one with an electrochemical quartz crystal microbalance (EQCM) combined with a jet impingement setup. The details of these experimental methods are described in the following section.

### SEM observation of iron carbonate dissolution

#### Test setup

A mild steel specimen was used to form an iron carbonate layer in a glass cell with a CO<sub>2</sub> solution supersaturated with respect to iron carbonate. It was then transferred and observed in a SEM. Periodically the specimen was immersed into a beaker filled with a CO<sub>2</sub> solution undersaturated with respect to iron carbonate, to make it dissolve the iron carbonate layer formed on the mild steel specimen. The SEM was used to observe the change of the appearance of the iron carbonate layer periodically and EDS was used to characterize the composition of the layer.

### Test matrix

The test matrix for the observation of iron carbonate dissolution using SEM is shown in Table 1.

Table 1. Text matrix for the observation of iron carbonate layer dissolution using SEM.

Parameters	Layer formation	Layer dissolution
Material	C1018	
Solution	1 wt% NaCl	
Temperature	80°C	25°C
CO <sub>2</sub> partial Pressure	0.52 bar	0.96 bar
Solution pH	6.6	3.8
Initial [Fe <sup>2+</sup> ]	50 ppm	0
Initial saturation level	300	0

### Test procedure

The iron carbonate layer formation was conducted on a flat mild steel specimen in a 2 liter glass cell with CO<sub>2</sub> saturated 1 wt% NaCl at 80°C. The temperature of the test solution was controlled by immersing a probe connected to a heater controller. CO<sub>2</sub> gas inlet and outlet were used to purge CO<sub>2</sub> gas before and during the test to maintain a saturated CO<sub>2</sub> corrosion environment. A pH probe was immersed into the solution to monitor the pH change during the test. The ferrous iron concentration was measured by taking samples of the test solution and using a spectrophotometer. Once the iron carbonate layer formation was finished, the specimen was taken from the glass cell and rinsed with isopropyl alcohol and dried.

A 1 wt% NaCl test solution (100 ml) was used for the iron carbonate layer dissolution which was prepared and deoxygenated with CO<sub>2</sub> in advance.

### **Glass cell with a rotating cylinder electrode setup**

#### Test setup

A glass cell with a rotating cylinder electrode (RCE) setup was used for the second part of the iron carbonate dissolution study. Many of the experimental details are the same as described in the section above. The schematic of the setup is shown in Figure 1, which was a three electrode system. A saturated Ag/AgCl electrode connected with Luggin capillary was used as the reference electrode. A concentric ring made from platinum wire served as the counter electrode. The working electrode was a cylindrical mild steel specimen with 5.4 cm<sup>2</sup> exposed surface area. It was mounted onto a shaft that can rotate at different speeds by connecting to a motor. Another identical test specimen was mounted onto a stationary shaft at the beginning of the test and immersed together with the RCE specimen. They were removed together from the solution after the layer formation process, and the stationary specimen was inspected by scanning electron microscope (SEM) to confirm the repeatability of the layer formation process. It was also used to compare with the RCE specimen, which was taken through a layer removal procedure.

A potentiostat was used to make electrochemical measurements during the test. The open circuit potential (OCP) was monitored and corrosion rate (CR) was measured using the linear polarization resistance (LPR) technique. Electrochemical impedance spectroscopy (EIS) was used to measure the solution resistance in order to estimate the corrosion resistance of the working electrode more accurately.

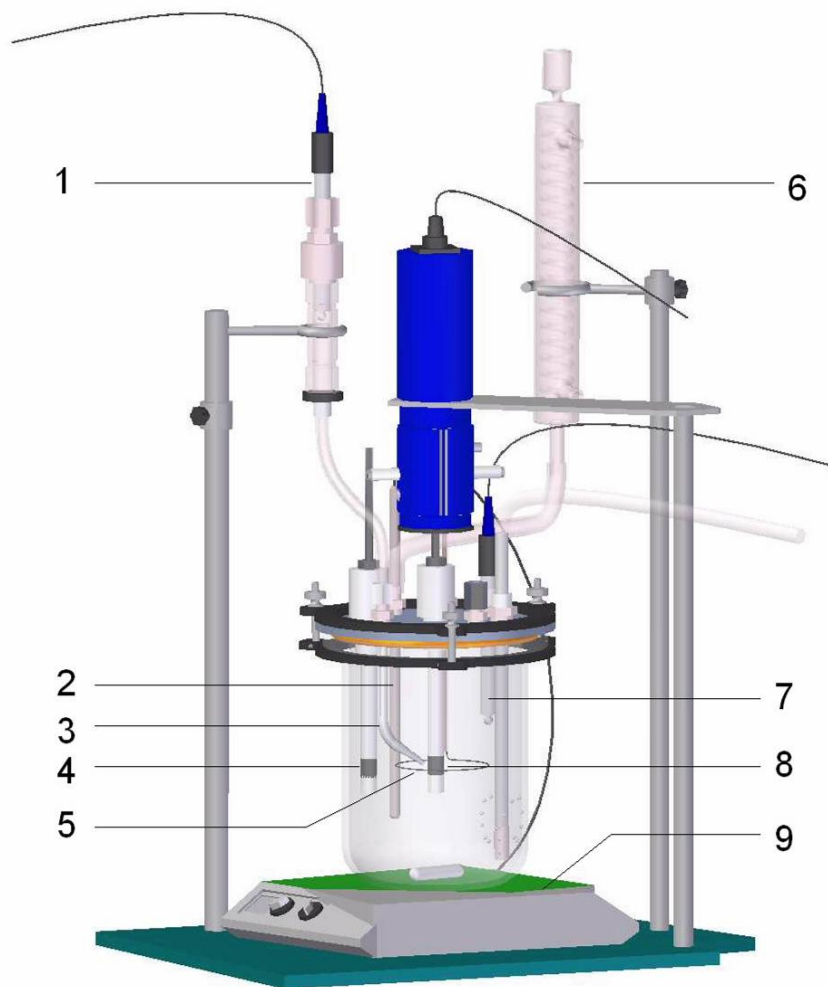


Figure 1. Schematic of glass cell with rotating cylinder electrode setup.  
1-reference electrode; 2-temperature probe; 3-Luggin capillary; 4-stationary cylindrical specimen; 5-counter electrode; 6-condenser; 7-pH probe; 8-working electrode (rotating cylindrical specimen); 9-heater/stirrer plate.

### Test matrix

The test matrix of iron carbonate dissolution conducted in a glass cell with rotating cylinder electrode setup is shown in Table 2.

Table 2. Text matrix for iron carbonate layer dissolution in a glass cell with a rotating cylinder electrode setup.

Parameters	Layer formation	Layer dissolution
Material	C1018	
Solution	1 wt% NaCl	
Temperature	80°C	
CO <sub>2</sub> partial Pressure	0.52 bar	
pH	6.6	5.6
Initial saturation level	300	0.3
Rotating speed	0	100 rpm

### Test procedure

A test solution was prepared in a glass cell by adding 1 wt% of NaCl into 2 liters of de-ionized water. After being well mixed, the test solution was deoxygenated by continuously purging a CO<sub>2</sub> gas for at least 2 hours before the test was started. At the same time, the solution was heated to 80°C. After the desired temperature was achieved, the pH of the test solution was adjusted to the designated value. The cylindrical C1018 test specimens were polished with 200, 400, 600 grit sand paper sequentially and simultaneously cooled by spraying with isopropyl alcohol. The two test specimens were washed with deionized water and isopropyl alcohol in an ultrasonic cleaner after polishing and dried with a blower. One test specimen was mounted on the shaft of the rotator and the other specimen was used as a stationary specimen. The test specimens were then immersed into the prepared test solution.

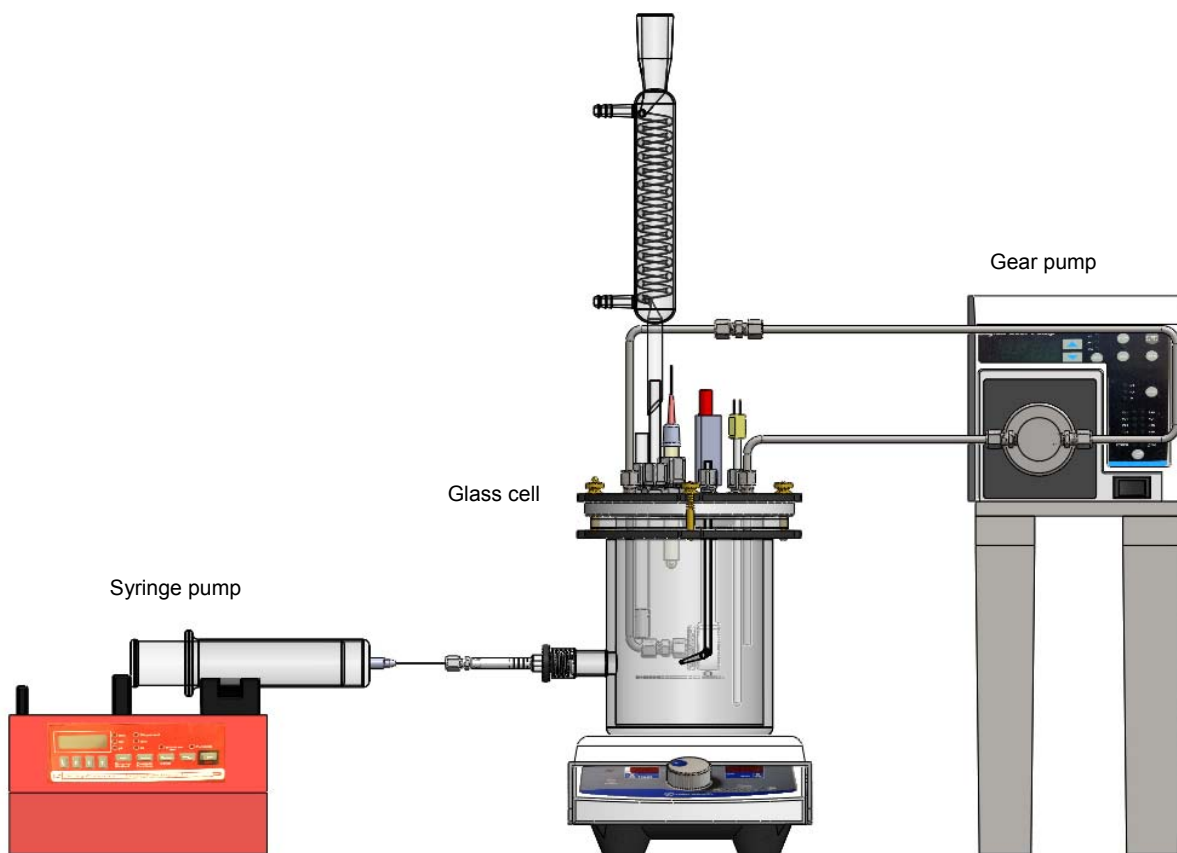
In order to accelerate the iron carbonate layer formation process, the ferrous ion concentration in the test solution was raised initially by adding a deoxygenated FeCl<sub>2</sub>·4H<sub>2</sub>O solution to increase the supersaturation level of iron carbonate. Corrosion rate of the working electrode was monitored using LPR continuously during the test as iron carbonate was precipitating on the steel surface. When the corrosion rate became stable and was below 0.1 mm/year, the layer formation process was deemed finished. The stationary specimen was removed from the solution and rinsed with isopropyl alcohol, dried and stored properly for surface analysis using SEM.

The solution pH was then decreased to the desired value by adding a deoxygenated HCl solution. The rotating cylinder electrode was gently rotated at 100 rpm to develop a well-defined flow condition. The corrosion rate and the corrosion potential were measured continuously during iron carbonate dissolution process. The solution pH and ferrous ion concentration were also monitored periodically. At the end of the test, the specimen was taken out, rinsed and dried for surface analysis.

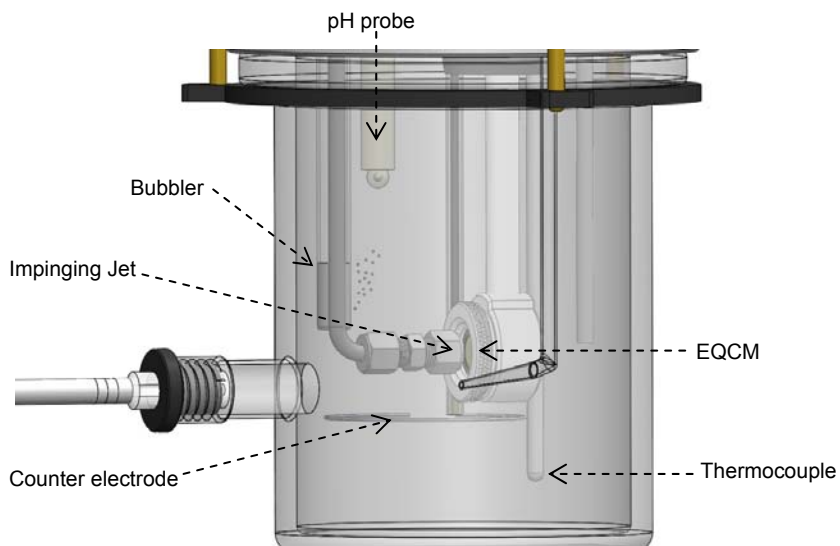
### **Glass cell with the electrochemical quartz crystal microbalance in a jet impingement setup**

#### Test setup

The glass cell setup with an EQCM and a jet impingement is shown in Figure 2. Unpolished platinum crystal was used in the tests. Details of the EQCM can be found elsewhere<sup>18</sup>. The parts in the glass cell were similar to those of the glass cell with RCE setup. A gear pump was used to circulate the test solution from the glass cell and create an impinging jet flow on the quartz crystal surface. The nozzle of the jet was 1 mm and the distance between the jet nozzle and the EQCM surface was 5 mm. In order to adjust the solution pH slowly during the dissolution test, a syringe pump was connected to the glass cell through a side port.



(a) The complete setup



(b) Enlarged view of the glass cell with the EQCM and the jet impingement arrangement.

Figure 2. Schematic of the glass cell setup with EQCM and jet impingement.

## Test matrix

The test matrix of iron carbonate layer formation and dissolution on a platinum coated quartz crystal is shown in Table 3.

Table 3. Test matrix for the iron carbonate layer formation and dissolution on a platinum coated quartz crystal.

Parameter	Layer formation	Layer dissolution
Material	Unpolished platinum coated quartz crystal	
Solution	1 wt% NaCl	
CO <sub>2</sub> partial pressure	0.52 bar	
Temperature	80°C	
pH	6.6	5.0 to 6.0
Initial S of FeCO <sub>3</sub>	300	<0.1

## Test procedure

Before conducting any tests with the EQCM, platinum quartz crystals were initially cleaned by acetone in an ultrasonic bath. Deionized water and isopropyl alcohol were then used to further clean the crystal surface. The crystal was installed in the EQCM holder and put into a two liter glass cell with 0.5 M H<sub>2</sub>SO<sub>4</sub> solution purged with N<sub>2</sub>. The potentiostat was used to polarize the platinum crystal at -1.2 V for 5 minutes to clean and activate the electrode. The crystal was then removed from the H<sub>2</sub>SO<sub>4</sub> solution and rinsed with deionized water. Another glass cell with two liters of 1 wt% NaCl solution was prepared and deoxygenated with CO<sub>2</sub> for 2 hours. This aqueous solution was heated to 80°C. Once the temperature was stable, the pH of the solution was adjusted to 6.6 by addition of a deoxygenated NaHCO<sub>3</sub> solution. The EQCM probe with the cleaned platinum quartz crystal was inserted into the solution and polarized at -700 mV for 30 minutes. Additional Fe<sup>2+</sup> ions were introduced into the glass cell by injecting a deoxygenated FeCl<sub>2</sub>·4H<sub>2</sub>O solution to create an iron carbonate supersaturation value of approximately 300 which was required to accelerate iron carbonate layer precipitation. Whether this adjustment was done before or after the EQCM sample was introduced, resulted in two different morphologies of iron carbonate, what will be discussed later. The Fe<sup>2+</sup> concentration and pH of the solution were periodically monitored during layer formation. After 24 hours or when the mass change on the EQCM stabilized, the layer formation was considered to be complete. A jet flow was then started to create a well-defined flow condition on the specimen surface. The solution pH was adjusted by adding a deoxygenated diluted HCl solution to reach an undersaturated condition and initiate dissolution. During the dissolution process, the solution pH and ferrous ion concentration were monitored regularly. The test was considered to be finished when the mass of the layer as detected by the EQCM became stable.

## **RESULTS AND DISCUSSION**

### **Iron carbonate dissolution observed by SEM**

The specimen surface after iron carbonate layer formation was first observed by SEM and characterized by EDS as shown in Figure 3. An evenly covered iron carbonate layer was obtained (formed at pH 6.6, 80°C, and SS (FeCO<sub>3</sub>)>>1). A number of larger prismatic crystals are present along with many smaller plate-like crystals. A set of iron carbonate dissolution observations was then made by SEM using a test solution with pH 3.8. This is an equilibrium pH when the water is saturated with 1 bar CO<sub>2</sub> at room temperature.

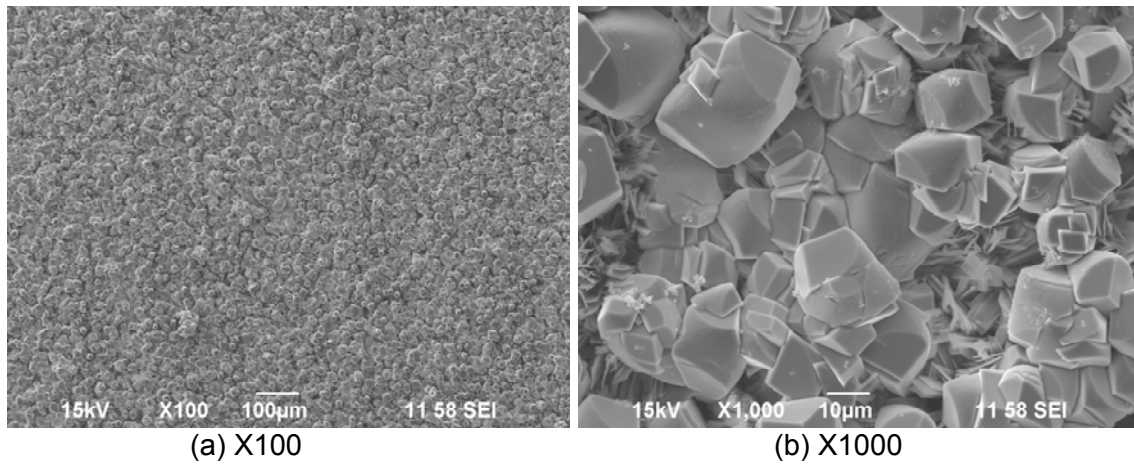


Figure 3. SEM images of the specimen surface after iron carbonate layer formation at pH 6.6, 1 wt% NaCl and 80°C.

The SEM images of the specimen shown in Figure 4 were taken after 15 hours of immersion in the undersaturated solution at pH 3.8. It can be clearly seen that many iron carbonate crystals disappeared from the surface due to dissolution. All the plate-like crystals are gone, suggesting that they are either easier to dissolve. According to the EDS analysis, the voids between the crystals only showed iron, which means the bare steel surface was exposed after dissolution.

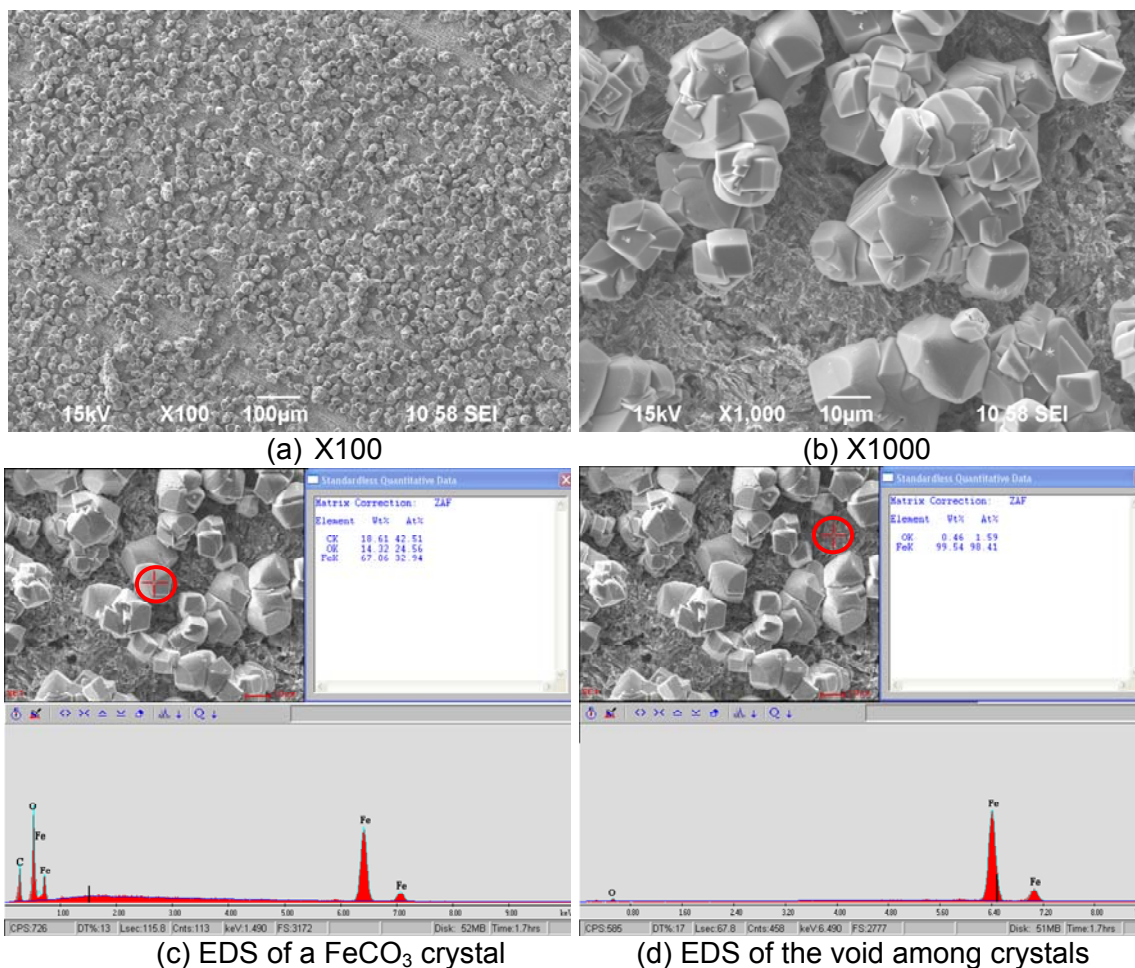


Figure 4. SEM and EDS images of the specimen surface after dissolution by pH 3.8 test solution for 15 hours.

Many similar experiments were repeated at different conditions and it was concluded that, while the observations by SEM gave some insight into the dissolution of iron carbonate layer, these were only qualitative results with limited practical value. Quantitative characterization of iron carbonate dissolution needed to be done in order to understand the kinetics and the important factors that control it.

### Iron carbonate layer formation and dissolution in a glass cell with a rotating cylinder electrode setup

Figure 5 shows the change of corrosion rate and corrosion potential in one of the dissolution tests conducted in a glass cell with a RCE setup. A protective iron carbonate layer was formed under a high initial supersaturation (pH 6.6, 80°C, and SS ( $\text{FeCO}_3$ )  $\gg 1$ ). Corrosion rate decreased due to the formation of a protective layer. The corrosion potential first decreased indicating formation of a diffusion barrier for cathodic species and then increased due to coverage of the surface and blockage of the anodic iron dissolution reaction. When the pH of the solution was adjusted to achieve an under-saturation level of 0.3, the corrosion potential decreased and corrosion rate increased immediately, which indicated the loss of protection by the iron carbonate layer due to dissolution.

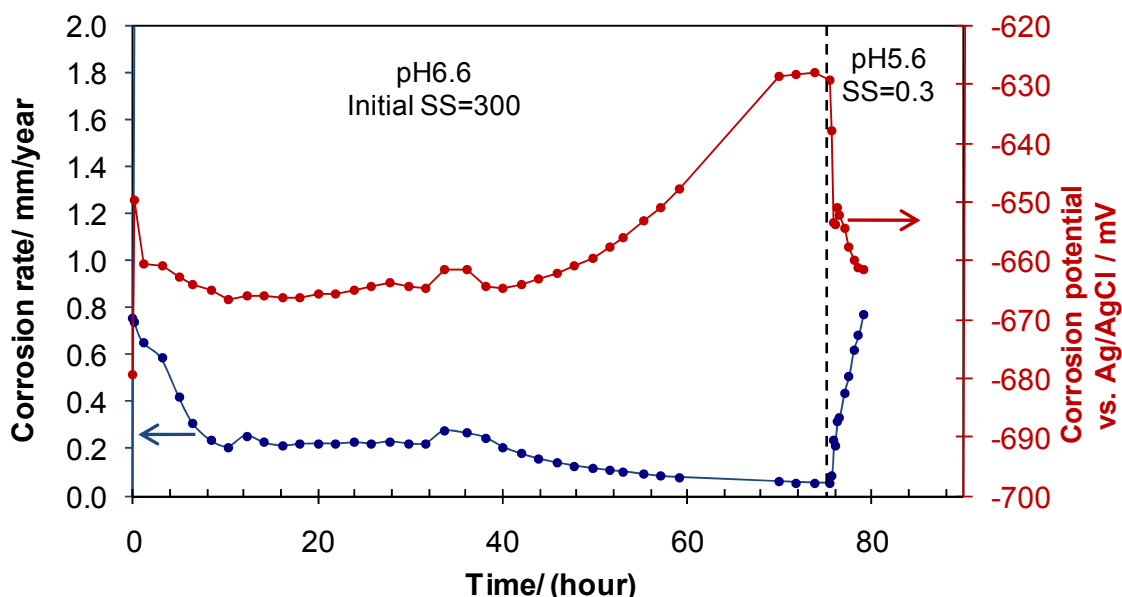
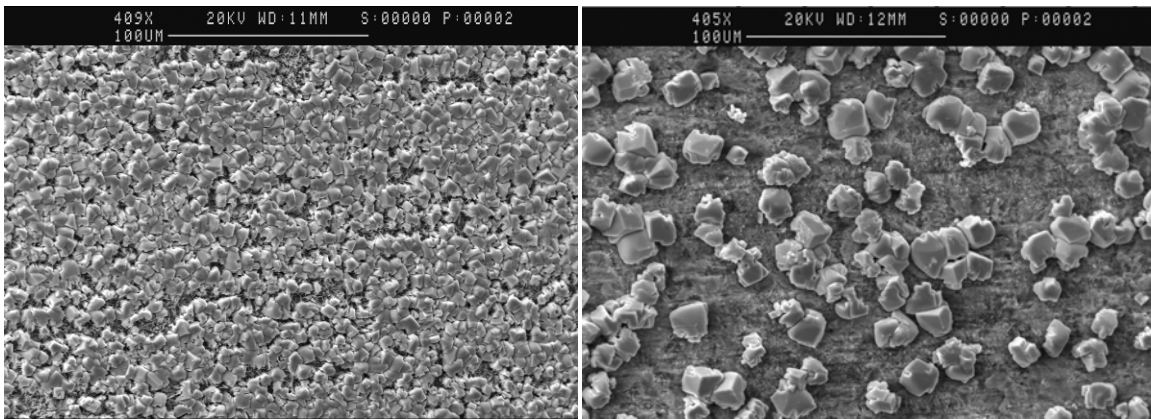


Figure 5. Change of corrosion rate (measured by LPR) and corrosion potential, during iron carbonate layer formation (pH 6.6, initial S=300, stagnant) and dissolution (pH 5.6, initial S=0.3, 100 rpm) in 1 wt% NaCl at 80°C. Test was conducted with a RCE glass cell setup.

SEM images taken before (when layer formation was finished) and after the dissolution process are shown in Figure 6. It can be seen that there was a protective layer formed on the surface of the steel specimen before the dissolution took place. After dissolution, many iron carbonate crystals were gone and the underlying steel substrate was exposed, which was the cause of the corrosion rate increase observed during the test. Tests using the same procedure were also conducted at different pH for iron carbonate dissolution process and a similar phenomenon was observed.



(a) X400 before dissolution

(b) X400 after dissolution

Figure 6. SEM images of the iron carbonate layer formed on mild steel, a) before dissolution (pH 6.6, initial  $S=300$ , stagnant) and after dissolution (pH 5.6, initial  $S=0.3$ , 100 rpm) in 1 wt% NaCl at 80°C. Test was conducted with RCE glass cell setup.

Although the findings obtained from the RCE tests seemed to be valid, they did not constitute a direct measurement of iron carbonate layer dissolution. The change of corrosion rate and corrosion potential were the consequences of dissolution, but not the ideal parameters to quantify the dissolution process. By using an electrochemical quartz crystal microbalance, the mass change due to the dissolution of the protective iron carbonate layer could be directly monitored, so it was selected as the most suitable technique, in the current study.

#### **Iron carbonate layer formation and dissolution in a glass cell with an electrochemical quartz crystal microbalance and a jet impingement setup**

Figure 7 shows the mass change monitored by EQCM during a iron carbonate layer precipitation and dissolution using a platinum coated quartz crystal substrate. The platinum surface was initially polarized to -700 mV vs. saturated a Ag/AgCl electrode which is close to the corrosion potential of a mild steel specimen under the same condition. After being polarized for 30 minutes, ferrous ions were injected into the solution to achieve a highly supersaturated condition with respect to iron carbonate ( $S>1000$ ). A rapid increase in mass attached to the EQCM was observed due to the precipitation of iron carbonate on the surface over the first 20 hours. Simultaneously, the saturation level decreased due to the consumption of the ferrous ions by precipitation. SEM images were taken after the iron carbonate layer formation stage, in order to check the morphology of the layer, and is shown in Figure 8. It can be seen from the image that a very compact layer of iron carbonate was formed on the platinum surface, similar in appearance to the one formed on mild steel (see Figure 6).

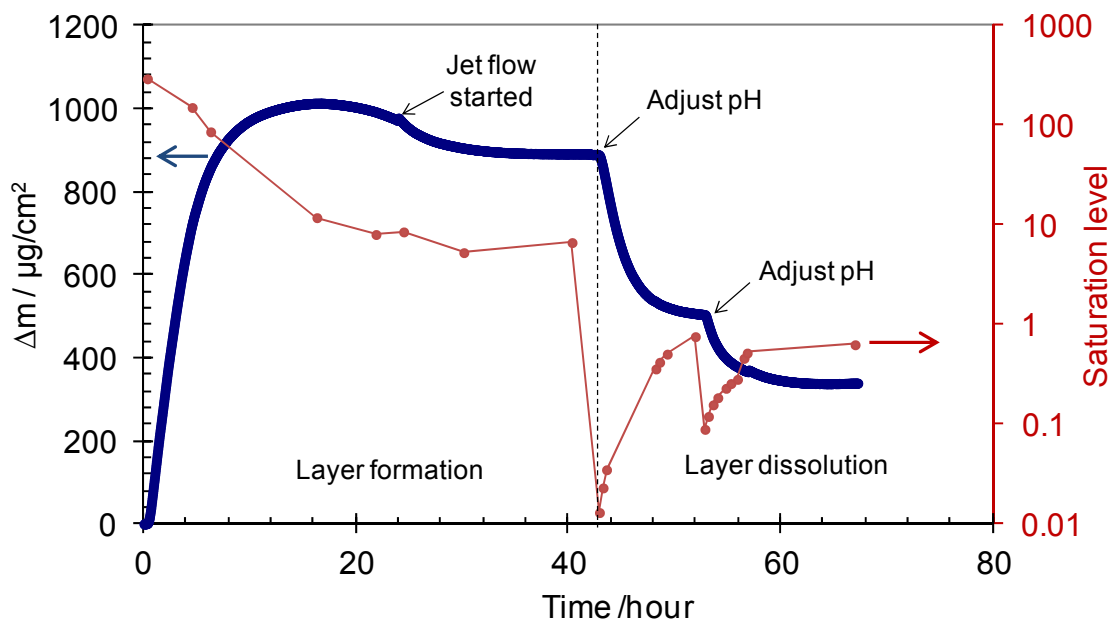


Figure 7. Mass change on the platinum quartz crystal monitored by EQCM in an iron carbonate layer formation and dissolution test; layer formation stage: pH 6.6, initial SS=300, stagnant; layer dissolution stage: pH 5.0~5.5, 80°C, 1 wt% NaCl, jet flow rate 1.3 m/s.

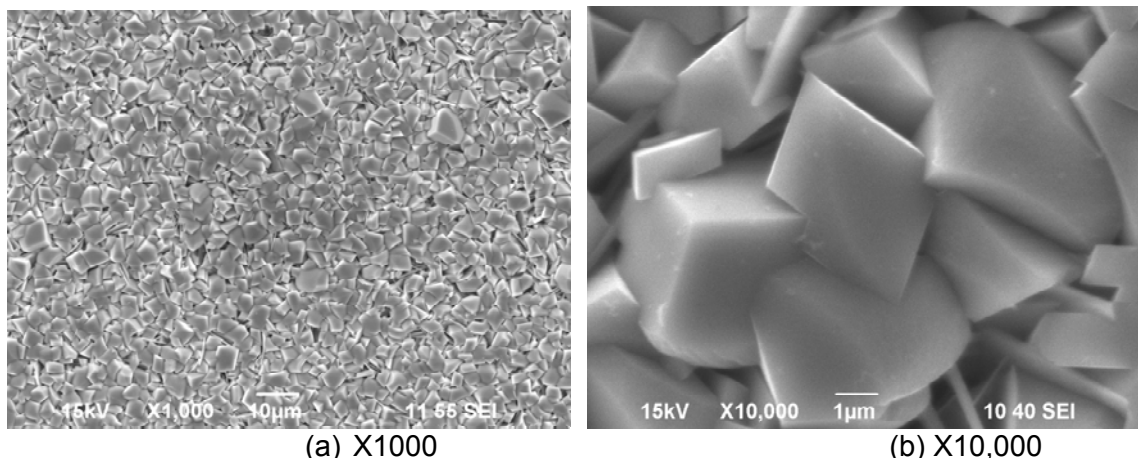


Figure 8. SEM images of EQCM specimen surface after iron carbonate layer formation on platinum coated quartz crystal substrate, 1 wt% NaCl, pH 6.6, initial SS=300, 80°C, platinum polarized to -700 mV vs. saturated Ag/AgCl electrode, stagnant conditions.

When the mass gain due to precipitation stopped (at approximately 24 h), an impinging jet flow at 1.3 m/s was started. The mass detected by the EQCM slightly decreased due to the change of the flow condition and then stabilized, as a small fraction of the iron carbonate was mechanically removed from the layer. The pH of the solution was then adjusted to a lower value to create an undersaturated condition with respect to iron carbonate. Immediate mass loss was detected by the EQCM due to iron carbonate dissolution, accompanied by the increase in ferrous ion concentration in the solution which approached the equilibrium saturation level of 1. In the experiment shown in Figure 7, the saturation level was decreased once more, with similar results.

Figure 9 shows the SEM and EDS images of the EQCM surface after the dissolution test. As can be seen in these images, most of the iron carbonate crystals were dissolved away and only some

remnants of iron carbonate crystals remained on the specimen surface. Some platinum substrate was exposed due to iron carbonate layer dissolution.

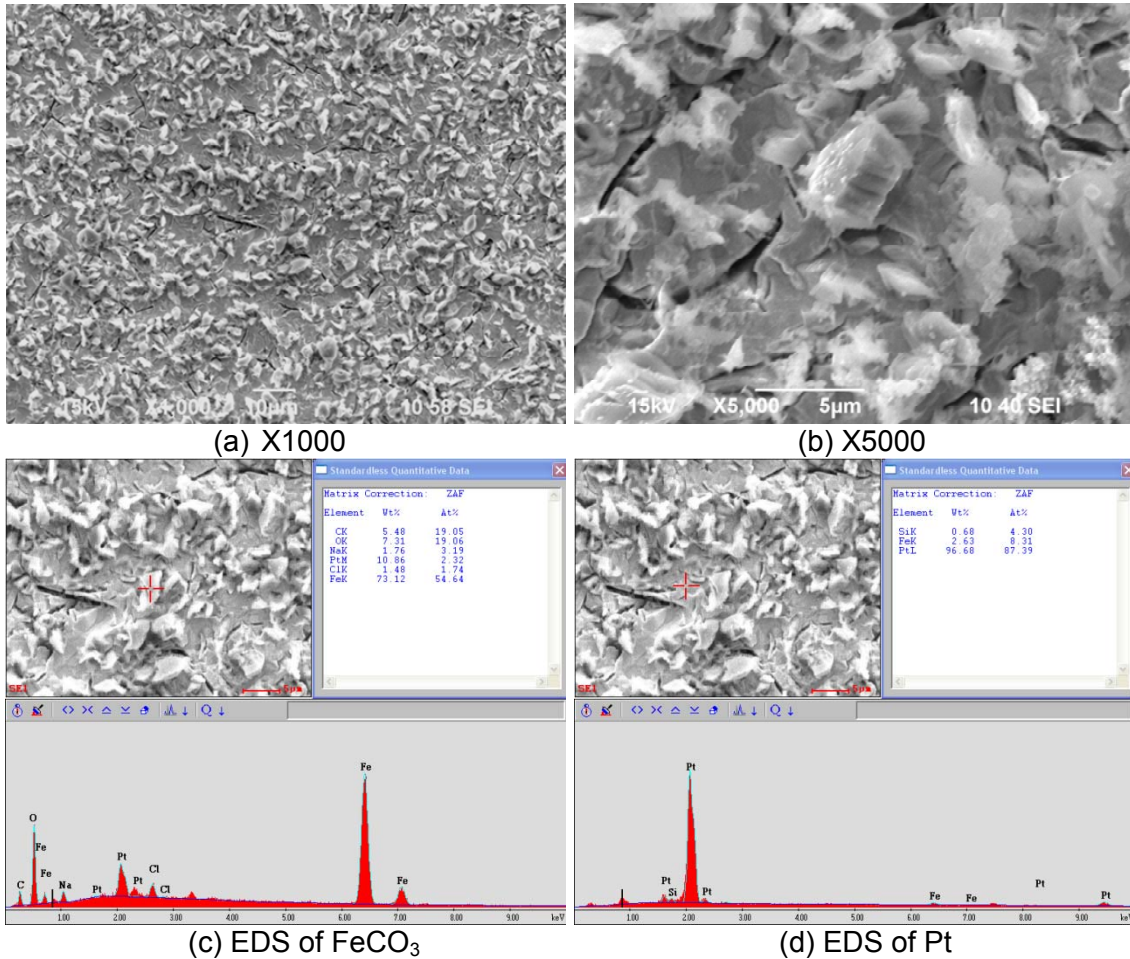


Figure 9. SEM and EDS images of the EQCM specimen surface after the iron carbonate (shown in Figure 8) dissolved, at pH 5.0~5.5, 80°C, 1 wt% NaCl, jet flow rate 1.3 m/s.

### Proposed mechanism of iron carbonate layer dissolution

Many different experiments of this kind were conducted at various conditions. From the EQCM measurements, the dissolution rate of iron carbonate can be obtained by calculating the slope of the mass change curve. The corresponding saturation level of solution with respect to iron carbonate during the dissolution process was calculated based on the systematic measurement of pH and ferrous ion concentration.

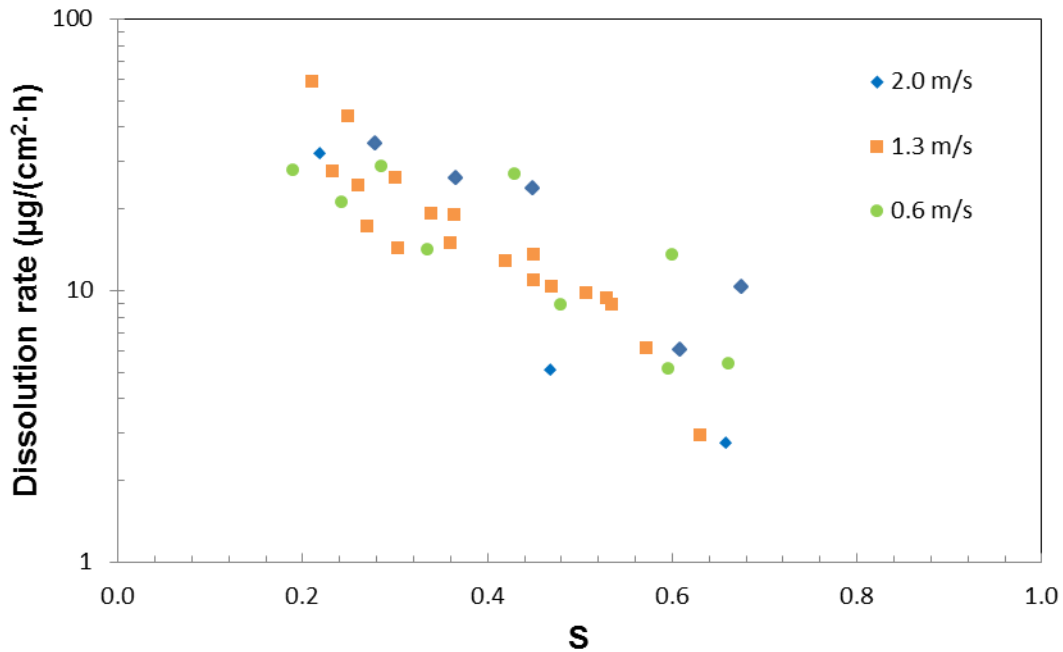


Figure 10. Dissolution rate change versus saturation level of iron carbonate as monitored by EQCM with platinum coated quartz crystal; 80°C, 1 wt% NaCl, different jet velocity in separate experiments.

Experiments conducted at different jet flow velocity, were done in order to examine the effect of mass transfer on the dissolution process. The dissolution rates from those tests are plotted versus saturation level in Figure 10. It can be seen that generally the dissolution rate increases with the level of undersaturation, as expected. It can also be seen that the change of jet velocity did not lead to any systematic effect on iron carbonate dissolution rate. This suggests that the dissolution process does not depend on the mass transfer rate, rather it is an indication of a surface reaction controlled process.

Previous studies on siderite dissolution, made in the geological field, proposed two parallel reactions for iron carbonate dissolution<sup>14,15</sup>:



When the solution is far from equilibrium ( $S \ll 1$ ), the overall dissolution rate can be described by:

$$r = k_{f1}c_{H^+}^n + k_{f2} \quad (5)$$

where  $r$  is the overall reaction rate of iron carbonate dissolution,  $k_{f1}$  and  $k_{f2}$  are the forward reaction rate constants of reactions (3) and (4) respectively,  $n$  is the order of the reaction.  $c_{H^+}$  is the concentration of  $H^+$ .

When the solution pH is higher, Equation (5) could not be used to characterize the dissolution process as the backward (precipitation) reactions must be considered. In this case, the overall reaction rate can be expressed as:

$$r = k_{f1}c_{H^+} - k_{b1}c_{Fe^{2+}}c_{HCO_3^-} + k_{f2} - k_{b2}c_{Fe^{2+}}c_{CO_3^{2-}} \quad (6)$$

where  $k_{b1}$  and  $k_{b2}$  are the backward reaction rate constants of reactions (3) and (4) respectively.  $c_{Fe^{2+}}$ ,  $c_{HCO_3^-}$  and  $c_{CO_3^{2-}}$  are the concentrations of  $Fe^{2+}$ ,  $HCO_3^-$  and  $CO_3^{2-}$ .

It was also pointed out that when pH was above 5.0, dissolution of iron carbonate is not pH-dependent<sup>14</sup> and dissolution of iron carbonate was dominated by reaction (4). The current study was done at a pH level 5.0 to 6.0 at 80°C, when the contribution from the backward reaction of reaction (4) also became significant. Therefore, only reaction (4) was considered in this study for characterizing the iron carbonate dissolution kinetics. So, the dissolution rate can be expressed as:

$$r = k_{f2} - k_{b2}c_{Fe^{2+}}c_{CO_3^{2-}} \quad (7)$$

After transformation, Equation (7) can be written as:

$$r = k_{f2}(1 - S) \quad (8)$$

$$\log(r) = \log(k_{f2}) + \log(1 - S) \quad (9)$$

Therefore, the parameters of the dissolution kinetics expression can be obtained by fitting the slope and intercept of the line ( $\log(r) \sim \log(1-S)$ ). As shown in Figure 11, the parameters in Equation (9) can be obtained by linear regression. The dissolution kinetics expression for iron carbonate were found to be:

$$r = (0.0045 \pm 0.0014)(1 - S)^{(2.3 \pm 0.5)} \quad (10)$$

where the unit of  $r$  is  $\text{mol} \cdot \text{m}^{-2} \cdot \text{h}^{-1}$ , and the unit of  $k_{f2}$  is also  $\text{mol} \cdot \text{m}^{-2} \cdot \text{h}^{-1}$ .

The order of reaction is approximately 2, which does not strictly follow either of the theoretical mechanisms (3) and (4) presented above. This type of 2<sup>nd</sup> order kinetics is rather common and suggests a more complex pathway for iron carbonate dissolution. Additional work is needed to elucidate the actual mechanism.

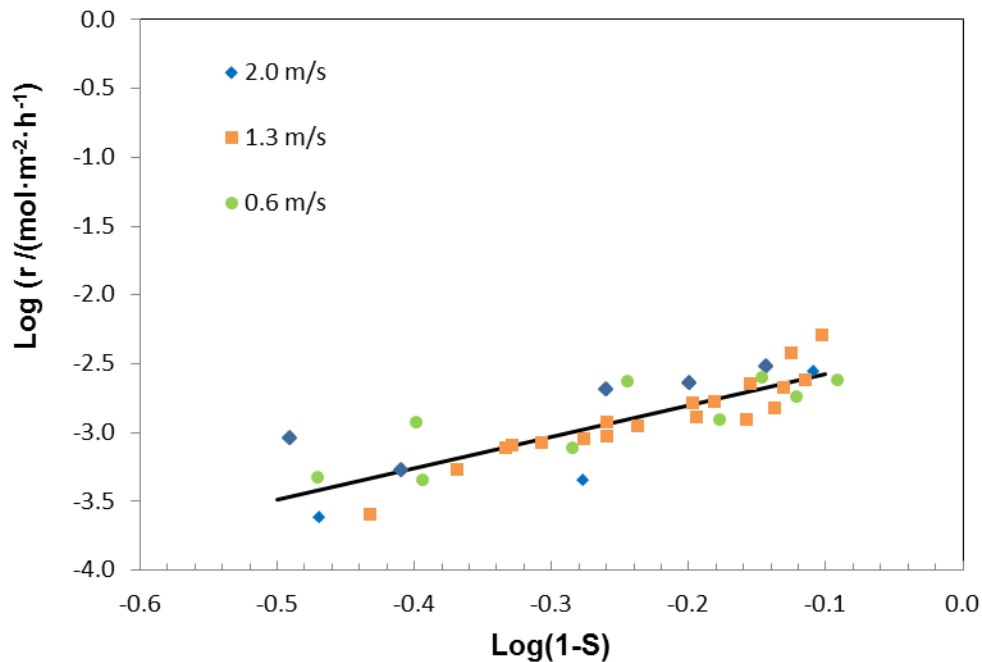


Figure 11. Dissolution rate change versus saturation level of iron carbonate as monitored by EQCM with platinum coated quartz crystal; 80°C, 1 wt% NaCl, different jet velocity in separate experiments.

The rates described by Equation (10) are valid for 80°C, in a 1 wt% NaCl aqueous solution. They are one to two orders of magnitude higher compared to the ones observed in the studies of siderite dissolution coming from the geological field<sup>6,12,14, 15,17</sup>. This can be explained by the different origin of iron carbonate, impurities as well as the differences in the experimental conditions (flow, saturation level, temperature, etc.).

## CONCLUSIONS

The dissolution behavior of iron carbonate was studied with different techniques.

- Qualitative observations conducted by using a SEM showed that the iron carbonate layer dissolved when exposed to an undersaturated condition, with the smaller plate-like crystal dissolving faster than the larger prismatic crystals.
- Quantitative tests conducted using an electrochemical rotating cylinder electrode setup, confirmed that the protective iron carbonate layer formed on steel surface could be damaged by dissolution and the corrosion rate increased as a result.
- Direct measurement of mass change using an electrochemical quartz crystal microbalance demonstrated that the dissolution rate of iron carbonate could be quantified directly. Results conducted at 80°C, in a 1 wt% NaCl aqueous solution, at different velocities indicate that there is no effect of mass transfer on iron carbonate dissolution.

## ACKNOWLEDGEMENTS

The financial support and technical directions from sponsoring companies: ConocoPhillips, BP, Eni, ExxonMobil, Petrobras, Saudi Aramco, Champion Technologies, Clariant, WGIM, NALCO, INPEX, Chevron, BG Group, ENCANA, PTT, PETRONAS, OXY, TransCanada, and Total are gratefully acknowledged.

## REFERENCES

1. Han, J., Brown, B., & Nescic, S. (2010). Investigation of the galvanic mechanism for localized carbon dioxide corrosion propagation using the artificial pit technique. *Corrosion*, 66(9), 1-12.
2. Yang, Y., Brown, B., Nescic, S., Gennaro, M., and Molinas, B., "Mechanical strength and removal of a protective iron carbonate layer formed on mild steel in CO<sub>2</sub> corrosion", *Corrosion/10*, paper No. 10383, Houston, TX, NACE 2010.
3. Dugstad, A. (1992). The importance of FeCO<sub>3</sub> supersaturation on the CO<sub>2</sub> corrosion of mild steels. Paper presented at the NACE Corrosion/92, paper no. 14.
4. Ruzic, V., Veidt, M., & Nescic, S. (2006). Protective iron carbonate films - Part 2: Chemical removal by dissolution in single-phase aqueous flow. *Corrosion*, 62(7), 598-611.
5. Duckworth, O. W., & Martin, S. T. (2004). Dissolution rates and pit morphologies of rhombohedral carbonate minerals. *American Mineralogist*, 89(4), 554-563.
6. Duckworth, O. W., & Martin, S. T. (2004). Role of molecular oxygen in the dissolution of siderite and rhodochrosite. *Geochimica et Cosmochimica Acta*, 68(3), 607-621.
7. Morse, J. W. (1983). The kinetics of calcium carbonate dissolution and precipitation. *Reviews in Mineralogy and Geochemistry*, 11(1), 227-264.
8. Morse, J. W., & Arvidson, R. S. (2002). The dissolution kinetics of major sedimentary carbonate minerals. *Earth-Science Reviews*, 58(1-2), 51-84.
9. Plummer, L. N., Parkhurst, D. L., & Wigley, T. M. L. (1979). Critical Review of the Kinetics of Calcite Dissolution and Precipitation Chemical Modeling in Aqueous Systems (Vol. 93, pp. 537-573): American Chemical Society.
10. Benezeth, P., Dandurand, J. L., & Harrichoury, J. C. (2009). Solubility product of siderite (FeCO<sub>3</sub>) as a function of temperature (25-250 °C). *Chemical Geology*, 265(1-2), 3-12.
11. Dresel, P. E. (1989). The dissolution kinetics of siderite and its effect on acid mine drainage. Doctoral Dissertation, Pennsylvania State University.
12. Golubev, S. V., Bénézech, P., Schott, J., Dandurand, J. L., & Castillo, A. (2009). Siderite dissolution kinetics in acidic aqueous solutions from 25 to 100 °C and 0 to 50 atm pCO<sub>2</sub>. *Chemical Geology*, 265(1-2), 13-19.
13. Greenberg, J., & Tomson, M. (1992). Precipitation and dissolution kinetics and equilibria of aqueous ferrous carbonate vs temperature. *Applied Geochemistry* 7, 185-190.
14. Pokrovsky, O. S., & Schott, J. (2002). Surface Chemistry and Dissolution Kinetics of Divalent Metal Carbonates. *Environmental Science & Technology*, 36(3), 426-432.
15. Testemale, D., Dufaud, F., Martinez, I., Benezeth, P., Hazemann, J.-L., Schott, J., et al. (2009). An X-ray absorption study of the dissolution of siderite at 300 bar between 50 °C and 100 °C. *Chemical Geology*, 259(1-2), 8-16.
16. van Cappellen, P., Charlet, L., Stumm, W., & Wersin, P. (1993). A surface complexation model of the carbonate mineral-aqueous solution interface. *Geochimica et Cosmochimica Acta*, 57(15), 3505-3518.
17. Tang, Y., & Martin, S. T. (2011). Siderite dissolution in the presence of chromate. *Geochimica et Cosmochimica Acta*, 75(17), 4951-4962.
18. Yang, Y., Brown, B., & Nescic, S. (2008). Application of EQCM to the study of CO<sub>2</sub> corrosion. Paper presented at the 17th International Corrosion Congress, paper no. 4071.